

Physics Contribution

Pareto Fronts in Clinical Practice for Pinnacle

Tomas Janssen, PhD, Zdenko van Kesteren, PhD, Gijs Franssen, PhD,
Eugène Damen, PhD, and Corine van Vliet, PhD

Department of Radiation Oncology, The Netherlands Cancer Institute, Amsterdam, The Netherlands

Received Jul 4, 2011, and in revised form May 1, 2012. Accepted for publication May 30, 2012

Summary

We show in detail how one can use Pareto fronts to perform an objective comparative treatment planning study in a clinically representative setting. To achieve this, we scripted our treatment planning system, Pinnacle, to generate thousands of plans per patient and developed a framework for the comparison. As an example, we compared volumetric modulated arc therapy (VMAT) with intensity modulated radiation therapy (IMRT) for prostate patients. Based on 60,000 generated plans, we found VMAT had a slight dosimetric advantage over IMRT.

Purpose: Our aim was to develop a framework to objectively perform treatment planning studies using Pareto fronts. The Pareto front represents all optimal possible tradeoffs among several conflicting criteria and is an ideal tool with which to study the possibilities of a given treatment technique. The framework should require minimal user interaction and should resemble and be applicable to daily clinical practice.

Methods and Materials: To generate the Pareto fronts, we used the native scripting language of Pinnacle³ (Philips Healthcare, Andover, MA). The framework generates thousands of plans automatically from which the Pareto front is generated. As an example, the framework is applied to compare intensity modulated radiation therapy (IMRT) with volumetric modulated arc therapy (VMAT) for prostate cancer patients. For each patient and each technique, 3000 plans are generated, resulting in a total of 60,000 plans. The comparison is based on 5-dimensional Pareto fronts.

Results: Generating 3000 plans for 10 patients in parallel requires on average 96 h for IMRT and 483 hours for VMAT. Using VMAT, compared to IMRT, the maximum dose of the boost PTV was reduced by 0.4 Gy ($P=.074$), the mean dose in the anal sphincter by 1.6 Gy ($P=.055$), the conformity index of the 95% isodose ($CI_{95\%}$) by 0.02 ($P=.005$), and the rectal wall $V_{65\text{ Gy}}$ by 1.1% ($P=.008$).

Conclusions: We showed the feasibility of automatically generating Pareto fronts with Pinnacle³. Pareto fronts provide a valuable tool for performing objective comparative treatment planning studies. We compared VMAT with IMRT in prostate patients and found VMAT had a dosimetric advantage over IMRT. © 2013 Elsevier Inc.

Introduction

Although in clinical practice there are strict dose criteria that need to be met, treatment planning is a subjective approach because quantification of the relative importance of organs at risk (OARs) and that of the target are clinically unknown. For a given patient,

there are many plans, all meeting clinical criteria but all with different relative sparing of the OARs. This subjectivity presents a problem for comparative treatment planning studies. If one compares 2 techniques based on 2 plans, one is never sure whether an observed difference is due to the different choices made for each plan or due to true differences between the techniques.

Reprint requests to: Corine van Vliet, PhD, Plesmanlaan 121, 1066 CX Amsterdam, The Netherlands. Tel: 31 20 512 2164; E-mail: c.v.vliet@nki.nl

Conflict of interest: none.

Pareto optimality can resolve this problem (1, 2). For a given set of parameters, a plan is called Pareto optimal if it is not possible to improve on all parameters simultaneously. The set of all Pareto optimal plans represents the Pareto front. By comparing the properties of the fronts, we compare all possible compromises between the evaluation parameters simultaneously, without the need to make a subjective choice as to what a good compromise is.

One way to study the Pareto front is by using multicriteria optimization (3-9). In implementing this approach in radiation therapy for a given patient a database of plans is generated automatically that approximates Pareto optimal plans. This database can then be presented to a dosimetrist, who can select the most appropriate plan for this patient. Although this is an interesting approach, the clinical feasibility of which has been shown (9), in practice most treatment planning systems offer a single objective, as there is only one cost function that the optimization tries to minimize.

To find the Pareto front by using single-objective optimization, one generates several plans and then constructs the Pareto front from those plans. This is a labor-intensive approach, and studies of this topic (1, 2, 10) typically generate only a limited number of plans, which are compared using 2-dimensional Pareto fronts. Although this certainly provides interesting information, the scope is typically too limited to be clinically relevant. In this work, we aimed for a full exploitation of the Pareto front in a clinically representative setting, using conventional treatment planning.

There were several issues we needed to take into account. First, one sets the planning objectives before optimization, while one can only evaluate the results of these objectives after optimization. (We distinguished between optimization objectives and evaluation objectives. The former are the objectives used by Pinnacle to optimize a plan, while the latter are the criteria on which a plan is clinically evaluated after optimization.) Therefore, in clinical practice, plans are generated in several iterations; each time changing some of the planning objectives, until the best compromise has been reached. Complicating the matter is the fact that in clinical practice, planning objectives are typically formulated as constraints (eg, maximum dose of less than X Gy), where the cost associated with such an objective becomes zero if the maximum dose is below X Gy. However, upon evaluation, parameters are required to be "as low as possible." Thus, in practice, there is not a one-to-one link between the planning objectives and the evaluation objectives.

Although theoretically this point can be overcome, in clinical practice it is not feasible to use conventional inverse planning to directly find the Pareto optimal plans. Because our aim was to provide a framework in a clinically representative setting, we generated plans similar to clinical practice: by changing the planning objectives. From the generated plans we then selected the Pareto front. To achieve this, we constructed a framework to generate the Pareto front, based on 3000 treatment plans, with various planning objectives, which are automatically generated using Pinnacle³ (Philips Healthcare, Andover, MA). All dose calculations, beam settings, and other factors conformed to clinical practice at the NKI-AVL.

As an example, we applied the framework to compare intensity modulated radiation therapy (IMRT) with volumetric modulated arc therapy (VMAT) for prostate cancer patients.

Methods and Materials

Hardware and software

Pareto plans were generated using Pinnacle³ version 9.0 software. The software runs on Sun OS version 5.10 and uses 4 Intel Xeon 2.93 GHz quad core processors.

We made extensive use of Pinnacle³'s native scripting language and Python script. Pareto fronts were constructed and evaluated using MatLab version 7.8.0 software.

Generating the plans

To generate many plans for a given patient, a script was written. The script does not require any user interaction. A flowchart showing the steps is given in Fig. 1. The patient is assumed to be "ready for planning," that is, all structures are delineated, beams are set up, and optimization parameters are set. Also, a starting set of planning objectives needs to be defined. In this work we used the settings and planning objectives that were used in the clinically delivered plan. Each iteration of new planning objectives are generated based on a "master set" of planning objectives. New objectives are drawn from a Gaussian distribution whose mean value is given by the master set and with a user defined (fixed) standard deviation. At the first iteration, the master is set to the initial set of planning objectives. After optimization, the plan is prescribed to the correct dose level, and all relevant data are saved. If the newly generated plan meets all clinical criteria and dominates the plan corresponding to the master set on at least all but one of the relevant evaluation parameters, the master set is changed to the new objectives. Dominance is not required on all evaluation parameters in order not to confine the search to a specific part of the Pareto front but, instead, allow the master set to "skim" alongside the Pareto front. If the master set is not changed for a given number of iterations, it is reset to the initial set. This is done to get a wider (clustered) approximation of the Pareto front.

Constructing the Pareto front

To generate the Pareto front, first, for each evaluation parameter, a range of clinically acceptable values is defined. All plans that

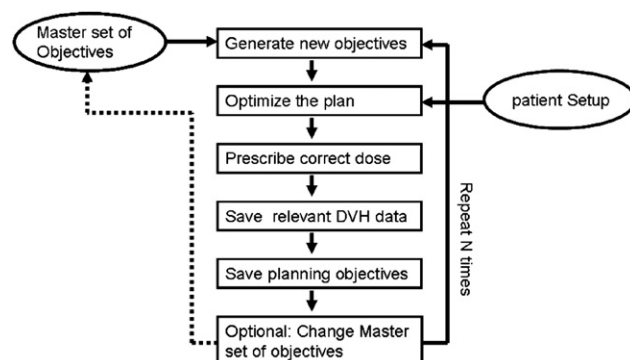


Fig. 1. Flowchart of the steps made by the script to automatically generate a large amount of plans.

violate these criteria are removed. From the remaining plans (Fig. 2A), the Pareto optimum is selected (Fig. 2B). We assumed that the Pareto front was convex and that the fact that the non-dominated set of points was not always convex was due to our finite sample size. Therefore, from the complete set of non-dominated plans, the convex subset was selected (Fig. 2C). Using linear interpolation, we constructed a convex surface (Fig. 2D). For Pareto fronts of more than 2 dimensions, the Pareto front is extrapolated, such that the Pareto front is defined over the complete (hyper)-cube bounded for each evaluation parameter by the minimum and maximum value of that parameter in the convex set of nondominated points. The front is extrapolated with points that dominate the original front by an infinitesimal amount (Fig. 2E, F). This extrapolation provides an upper boundary for the true Pareto front, and therefore it is guaranteed that the extrapolated points are physically achievable.

Comparing Pareto fronts

Two Pareto fronts can be compared in an objective way, provided that we do not assign a relative weight to the different evaluation parameters. This means that we cannot summarize the differences between 2 fronts in 1 single number but instead compare 2 fronts for each evaluation parameter separately. For a given evaluation parameter, we took, for each value of all other evaluation parameters, the difference between the 2 fronts. This set of differences we called the Pareto difference set (PDS) (Fig. 3). For each evaluation parameter, the differences between 2 Pareto fronts can be qualified and quantified using this set. Mathematically we can describe the PDS as follows. Suppose we have 2 n -dimensional Pareto fronts, P and L . The value of the fronts in dimension k is

$$P_k = P_k(\vec{x}); L_k = L_k(\vec{x}),$$

where \vec{x} is an $(n-1)$ -dimensional vector in the space spanned by all dimensions except k . For this dimension, the PDS is given by the union

$$PDS_k = \bigcup_{\vec{x} \in X} (P_k(\vec{x}) - L_k(\vec{x})),$$

where X is the set of all possible $(n-1)$ -dimensional vectors, for which both P_k and L_k are defined.

For each dimension, we considered the 3 quartiles (those points that divide a set into 4 groups of equal size) of the associated PDS, which we indicated by Ψ_1 , Ψ_2 and Ψ_3 . To quantify differences among the fronts, we used the median of the PDS, which is by definition Ψ_2 . Ψ_2 should be interpreted as the median difference between 2 Pareto fronts for a given dimension.

To qualify the difference, we need some measure to determine when we call 2 fronts “similar.” This measure, ϵ , we chose to be 5% of the range where the Pareto fronts were defined (Fig. 3) as,

$$\epsilon_k = 0.05(\max(P_k, L_k) - \min(P_k, L_k)),$$

We considered the PDS of P - L and recognized the 4 following qualifications of the difference between 2 Pareto fronts.

$$P < L: \Psi_1 < -\epsilon; \Psi_3 < +\epsilon$$

In this case (Fig. 3A, B), a substantial part of the Pareto P front lies lower than the Pareto L front (the first quartile is large and negative), while an insignificant part of P lies above L (the third quartile is not large and positive). P obtains a lower value and corresponds to the better technique.

$$P > L: \Psi_1 > -\epsilon; \Psi_3 > +\epsilon$$

This is the opposite of case 1. P obtains a higher value than L and corresponds to the lesser technique.

$$P \sim L: \Psi_1 > -\epsilon; \Psi_3 < +\epsilon$$

In this case (Fig. 3C, D), neither a substantial part of P lies lower than L (the first quartile is not large and negative), nor does a substantial part lie higher (the third quartile is not large and positive). P and L are therefore comparable.

$$P ? L: \Psi_1 < -\epsilon; \Psi_3 < +\epsilon$$

In this case (Fig. 3E, F), both a substantial part of P lies lower than L (the first quartile is large and negative), and a substantial part lies higher (the third quartile is large and positive). In such a case our qualification cannot be used to determine the better technique.

IMRT vs VMAT: patients and setup

As an example, we compared IMRT with VMAT for prostate cancer patients. Pareto fronts for 10 patients were analyzed. Conforming to clinical practice at the NKI-AVL (11), all patients were prescribed 2 dose levels: 72.2 Gy to the planning target volume (PTV) (clinical target volume [CTV] plus 7 mm) and 78 Gy to the boost PTV (CTV plus 4 mm). For 5 patients, the CTV equaled that of the prostate only, while for the other 5 patients, the CTV included the seminal vesicles. These patients are henceforth referred to as group 1 and 2, respectively.

All relevant planning parameters were identical to the ones used in clinical practice at the NKI-AVL. For the IMRT plans, a 5-beam setup with 10-MV beams was used. For the VMAT plans, a single 10-MV arc was used, rotating over 336°. For both techniques, optimization was done in 40 iterations. The first 10 were used to optimize the fluence maps (in Pinnacle³ both IMRT and VMAT optimization starts with fluence optimization), while the following 30 used direct aperture optimization.

For each patient and for each technique, 3000 plans were optimized, resulting in a total of 60,000 plans.

IMRT vs VMAT: planning objectives

As a master set of planning objectives, the planning objectives that were used in the clinically delivered plan were used. The same set was used both for VMAT and IMRT. Table 1 shows an example of planning objectives for group 1 patients. The set for group 2 patients is similar. Table 1 also shows the standard deviations (sigma) used to generate new sets of planning objectives. For each patient and for each technique, the same set of standard deviations was used.

IMRT vs VMAT: evaluation objectives

All plans were evaluated based on the the largest dose received by 1% of the volume ($D_{1\%}$) of the boost PTV (the $D_{99\%}$ of the boost PTV was not used, because all plans were automatically prescribed such that the $D_{99\%}$ [boost PTV] = 95%), the $D_{99\%}$ of the PTV, the volume receiving at least 75 Gy ($V_{75 \text{ Gy}}$), and $V_{65 \text{ Gy}}$ of the rectal wall, the mean dose to the anal sphincter (defined as the most caudal 3 cm of the rectum), the maximum dose to the femoral heads and the conformity index of the 95% isodose

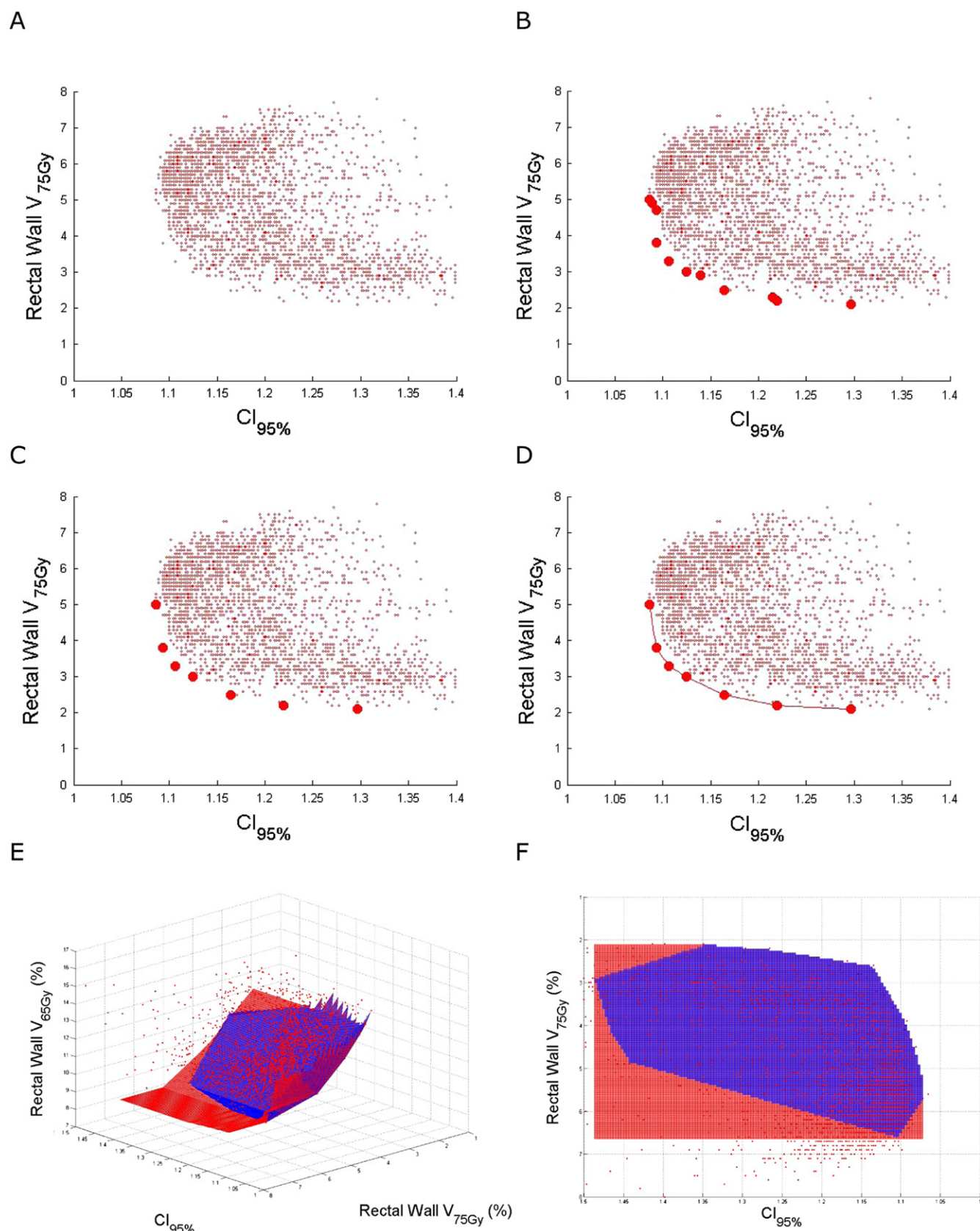


Fig. 2. Steps to generate a Pareto front. CI_{95%} is the conformity index of the 95% isodose and V_{x Gy} denotes the volume receiving at least X Gy. (A) Clinically acceptable plans. (B) Pareto optimal points. (C) The convex subset of the points. (D) A linear interpolation gives the Pareto front. (E) For more than 2 dimensions, an extrapolation of extreme values is performed. Dark blue is the original front; light red is the interpolation. (F) A top view of panel E.

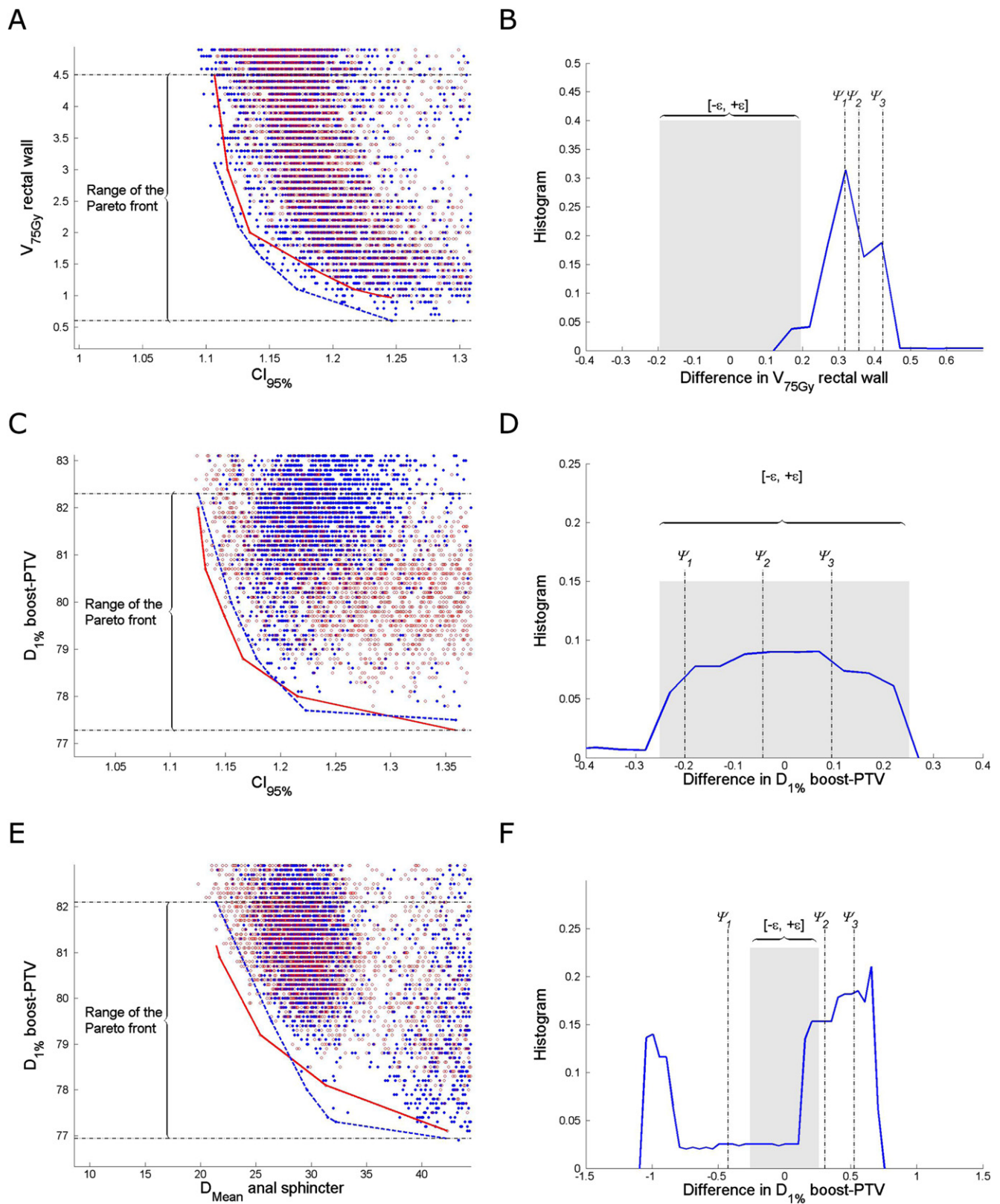


Fig. 3. Qualification of Pareto fronts using the PDS. The left figures show 2-dimensional Pareto fronts for IMRT (red, solid) and VMAT (blue, dashed), exemplifying different qualifications. The right figures show the histogram of the PDS of IMRT-VMAT. The epsilon range (gray) is 5% of the range of the Pareto front. The quartiles of the PDS are indicated by ψ_1 - ψ_3 . (A and B) Classification of VMAT < IMRT; (C and D) VMAT ~ IMRT; (E and F) VMAT? IMRT. Notice that these data are to be analyzed using a 5-dimensional Pareto front and that these plots are meant only for illustration.

Table 1 Planning objectives and standard deviations (sigma)

Site	Dose	Target dose (cGy)		Volume (%)		Weight	
		Value	Sigma	Value	Sigma	Value	Sigma
PTV	MinDose	7220	0			90	0
Boost-PTV	MinDose	7566	0			100	0
	Uniform dose	7800	0			10	0
	MaxDose	8190	0			50	0
	Max EUD (a = 1)	2150	1200			40	4
Rectal wall	Max EUD (a = 12)	6200	800			15	3
	Max EUD (a = 1)	1750	900			3	2
Anal sphincter	MaxDVH	7450	300	6	1	70	0
PTV minus boost-PTV	MaxDVH	6000	500	15	1	5	2
PTVring	MaxDVH	6350	500	5	1	5	2
	MaxDose	7050	500			5	2
	MaxDose	4950	0			20	3
Right femur	MaxDose	4950	0			20	3

Abbreviations: DVH = dose-volume histogram; EUD = equivalent uniform dose, with a volume parameter of a .

The PTV ring is a ring of 1 cm around the PTV. If no volume parameter is specified, that objective acts on the complete region of interest. The choices for the values of sigma have been made to best reflect the choices made by the dosimetrists in clinical practice. For example, the objectives of the PTV and the boost-PTV are typically not changed, and therefore, they get a sigma of zero.

($CI_{95\%}$) = [volume (95% isodose)]/[$V_{95\%}$ (PTV)]. Because all plans were prescribed on the $D_{99\%}$ of the boost PTV, target coverage was ensured by construction, and the $CI_{95\%}$ value is a proper measure of conformity. Similarly, the $D_{1\%}$ value was a measure of dose homogeneity in the boost PTV. Clinically acceptable plans were selected based on threshold values for all these parameters. However, we did not aim for a minimization of the maximum dose in the femoral heads but only required it to be less than 50 Gy. Similarly, the $D_{99\%}$ of the PTV was not maximized but only required to be at least 95% of 72.2 Gy. The 5 remaining parameters (the $D_{1\%}$ of the boost PTV, the $V_{75\text{ Gy}}$ and $V_{65\text{ Gy}}$ of the rectal wall, the mean dose in the anal sphincter, and the $CI_{95\%}$) are the parameters we wanted to minimize and therefore use for our Pareto analysis.

Analysis of IMRT vs VMAT

Our analysis was based entirely on 5-dimensional Pareto fronts. Our convention was to consider the PDS of IMRT-VMAT such that positive values of the PDS implied that the VMAT Pareto front lay below the IMRT Pareto front, and thus corresponded to the better technique. Statistical significance of the difference of Ψ_2 from zero was calculated using a t test.

Results

Comparison of the fronts

Tables 2 and 3 compare results of IMRT vs those of VMAT. We find from Table 2 that for all evaluation criteria, VMAT is in most cases superior or equivalent to IMRT. If we consider all data, VMAT is superior in 72% of cases, while IMRT is superior in 14% of cases. Per patient, we found that for 7 patients (3 in group 1, 4 in group 2) VMAT was superior or equivalent for all objectives, while only for 1 patient (group 1), IMRT was superior or equivalent for all evaluation objectives.

In Table 3, we report our quantitative results. Considering all patients, VMAT performed better than IMRT for all evaluation objectives. Significant differences were observed for the rectal wall $V_{65\text{ Gy}}$ ($\Psi_2 = 1.1\%$, $P = .008$) and the $CI_{95\%}$ ($\Psi_2 = 0.02$, $P = .005$). We found that for all evaluation objectives, the improvement was larger for group 2 than for group 1.

Efficiency of the approach

The optimization and dose calculation of 3000 plans required, on average, 96 hours (range, 85-106 h) for IMRT and 483 h (range, 405-534 hours) for VMAT.

We found that on average, 1242 (range, 182-2427) of the total number of generated plans were clinically acceptable. Of the acceptable plans, on average 133 (range, 44-204) were part of the convex Pareto set.

Table 2 Classification of the differences among Pareto fronts

Classification	Group 1 (n=5)				Group 2 (n=5)				All data (n=10)			
	<	~	>	?	<	~	>	?	<	~	>	?
Boost PTV max dose	3	0	2	0	4	0	0	1	7	0	2	1
Anal sphincter mean dose	2	1	2	0	5	0	0	0	7	1	2	0
$CI_{95\%}$	3	2	0	0	4	1	0	0	7	3	0	0
Rectal wall $V_{65\text{ Gy}}$	4	0	1	0	5	0	0	0	9	0	1	0
Rectal wall $V_{75\text{ Gy}}$	3	0	2	0	3	1	0	1	6	1	2	1

Abbreviations: $CI_{95\%}$ = conformity index of the 95% isodose.

Classification of the differences among Pareto fronts based on the PDS = Pareto difference set of IMRT-VMAT. The < sign implies that the VMAT Pareto front lies below the IMRT Pareto front and is thus superior, while the opposite is true for the > value. The ~ sign indicates both fronts are equivalent, while the ? sign indicates that no proper comparison can be made. The Table lists the number of patients who were classified for a specific evaluation objective.

Table 3 Quantification of Pareto front differences

Plan	Group 1 (n=5)			Group 2 (n=5)			All data (n=10)		
	Mean value	Mean Ψ_2	P	Mean value	Mean Ψ_2	P	Mean value	Mean Ψ_2	P
Boost PTV max dose (Gy)	78.8	0.2	.656	79.6	0.6	.028	79.3	0.4	.074
Anal sphincter mean dose (Gy)	15.1	0.4	.645	18.3	2.9	.050	16.7	1.6	.055
CI _{95%}	1.12	0.01	.034	1.17	0.02	.055	1.15	0.02	.005
Rectal wall V _{65 Gy} (%)	11.4	0.3	.393	15.5	1.7	.001	13.4	1.1	.008
Rectal wall V _{75 Gy} (%)	3.0	0.0	.999	3.5	0.3	.289	3.24	0.2	.414

The table shows quantification of the differences between the Pareto fronts based on the PDS of IMRT-VMAT, using the median difference between the 2 Pareto fronts, Ψ_2 . To summarize the data, we present the mean of Ψ_2 over all patients. *P* values were determined by using a 1-parameter *t* test with respect to zero. As a reference, we also present the mean value of the combination of both Pareto fronts. If Ψ_2 is positive, the VMAT Pareto front lies below the IMRT Pareto front.

Discussion

Efficiency and alternative approaches

Our approach was not very efficient because the number of Pareto optimal plans ranged only from 44–204. Craft et al (4) showed that the error in sampling a 6-dimensional Pareto front is <5% for 55 points. The sampling density of our 5-dimensional Pareto fronts then should be sufficient to obtain at least <5% error in all cases but one (explicit data not shown). More elaborate approaches might result in a more efficient generation of the Pareto front.

For example, one could use a genetic approach to generate new planning objectives (7). In that approach, combinations of good planning objectives are used to construct new planning objectives. Alternatively, according to an idea used by Craft et al (5), one could systematically scan the Pareto front by first focusing on the asymptotic values of each evaluation objective and then by interpolating (5).

We are working on implementing a technique by Bosman (12). In this approach, the search space of the planning objectives is iteratively aligned with the Pareto front of the evaluation objectives. Preliminary results indicate accurate results can be obtained (after a fast “training” of the optimizer using fluence map optimization) within 300 iterations.

Comparing Pareto fronts

Our Pareto front comparison provides a qualification and quantification of the better technique; however, some information is lost. If 1 technique dominates some part of the Pareto front while the other technique dominates elsewhere, our classification fails. Teichert et al (13) introduced a technique to compare Pareto fronts that gives some insight into such a situation. By projecting the difference between 2 fronts one learns where each front dominates. However, it appears hard to use this framework to quantify the differences in a clinically relevant way. A combination of the technique presented in reference 13 and the technique presented here might give additional insight into these cases.

Comparing IMRT with VMAT

We found that for 7 patients, the Pareto front of VMAT was superior or equivalent to the Pareto front of IMRT for all evaluation criteria, while the opposite was true only for 1 patient. Our quantitative analysis found significant differences of 0.02

(*P* = .005) for the CI_{95%} and 1.1 % (*P* = .008) for the rectal wall V_{65 Gy}, in favor of VMAT.

Several treatment planning studies comparing VMAT with IMRT have appeared in the literature (14–17). All these studies suffer from a subjectivity problem: for each technique, 1 single plan was compared per patient. All publications found, on average, a slight decrease of the dose delivered to the rectum for VMAT compared to that of IMRT: Kjeir-Kristoffersen et al (14) reported V_{60 Gy}/V_{70 Gy}, respectively, for the rectum, IMRT 12%, VMAT 8%; Palma et al (15) reported V_{70 Gy}, IMRT 4.1%, VMAT 3.6%; Tsai et al (16) reported V_{60 Gy} for the rectum, IMRT 14.7%, VMAT 12.4%; and Zhang et al (17) reported V_{75.6 Gy} for the rectum, IMRT 22%, VMAT 19.4%. A quantitative comparison with our results is not possible; however, qualitatively, we found similar results. For the CI_{95%}, Palma et al (15) found 1.12 for IMRT and 1.17 for VMAT, whereas Tsai et al (16) found 1.5 for IMRT and 1.6 for VMAT: 1.6. While the order of magnitude of the CI_{95%} was similar to what we found (mean value, 1.15), this contrasts with our statistically significant (*P* = .005) finding that VMAT produced more conformal plans than IMRT for 9 of 10 patients.

Conclusions

We implemented a framework to generate clinically relevant Pareto fronts in Pinnacle³. Generation of the fronts is fully automatic and therefore can be based on any number of plans. As an example, we used the fronts to compare IMRT with VMAT for prostate patients. The comparison does not depend on the subjective choice of which plans to compare, as hundreds of plans are compared simultaneously. We found that Pareto optimal VMAT plans are more conformal and provide better sparing of the rectum than Pareto optimal IMRT plans.

References

- Ottosson RO, Karlsson A, Behrens CF. Pareto front analysis of 6 and 15 MV dynamic IMRT for lung cancer using pencil beam, AAA and Monte Carlo. *Phys Med Biol* 2010;55:4521–4533.
- Ottosson RO, Engstrom PE, Sjostrom D, et al. The feasibility of using Pareto fronts for comparison of treatment planning systems and delivery techniques. *Acta Oncol* 2009;48:233–237.
- Craft D, Halabi T, Shih HA, et al. An approach for practical multi-objective IMRT treatment planning. *Int J Radiat Oncol Biol Phys* 2007;69:1600–1607.
- Craft D, Bortfeld T. How many plans are needed in an IMRT multi-objective plan database? *Phys Med Biol* 2008;53:2785–2796.

5. Craft DL, Halabi TF, Shih HA, et al. Approximating convex Pareto surfaces in multiobjective radiotherapy planning. *Med Phys* 2006;33:3399-3407.
6. Hoffmann AL, Siem AY, den Hertog D, et al. Derivative-free generation and interpolation of convex Pareto optimal IMRT plans. *Phys Med Biol* 2006;51:6349-6369.
7. Holdsworth C, Kim M, Liao J, et al. A hierarchical evolutionary algorithm for multiobjective optimization in IMRT. *Med Phys* 2010;37:4986-4997.
8. Monz M, Kufer KH, Bortfeld TR, et al. Pareto navigation: algorithmic foundation of interactive multi-criteria IMRT planning. *Phys Med Biol* 2008;53:985-998.
9. Thieke C, Kufer KH, Monz M, et al. A new concept for interactive radiotherapy planning with multicriteria optimization: first clinical evaluation. *Radiother Oncol* 2007;85:292-298.
10. Steneker M, Lomax A, Schneider U. Intensity modulated photon and proton therapy for the treatment of head and neck tumors. *Radiother Oncol* 2006;80:263-267.
11. Peeters ST, Heemsbergen WD, van Putten WL, et al. Acute and late complications after radiotherapy for prostate cancer: results of a multicenter randomized trial comparing 68 Gy to 78 Gy. *Int J Radiat Oncol Biol Phys* 2005;61:1019-1034.
12. Bosman PAN. The anticipated mean shift and cluster registration in mixture-based EDAs for multi-objective optimization. In: Branke J, Alba E, Arnold D, editors. Proceedings of the ACM Annual Genetic and Evolutionary Computation Conference. London, England: ACM Press, New York; 2010. p. 351-358.
13. Teichert K, Suss P, Serna JJ, et al. Comparative analysis of Pareto surfaces in multi-criteria IMRT planning. *Phys Med Biol* 2011;56:3669-3684.
14. Kjaer-Kristoffersen F, Ohlhues L, Medin J, et al. RapidArc volumetric modulated therapy planning for prostate cancer patients. *Acta Oncol* 2009;48:227-232.
15. Palma D, Vollans E, James K, et al. Volumetric modulated arc therapy for delivery of prostate radiotherapy: comparison with intensity-modulated radiotherapy and three-dimensional conformal radiotherapy. *Int J Radiat Oncol Biol Phys* 2008;72:996-1001.
16. Tsai CL, Wu JK, Chao HL, et al. Treatment and dosimetric advantages between VMAT, IMRT, and helical tomotherapy in prostate cancer. *Med Dosim* 2010.
17. Zhang P, Happersett L, Hunt M, et al. Volumetric modulated arc therapy: planning and evaluation for prostate cancer cases. *Int J Radiat Oncol Biol Phys* 2010;76:1456-1462.